Supplementary Information (SI) for Lab on a Chip.
This journal is © The Royal Society of Chemistry 2024

Electronically actuated artificial hinged cilia for efficient bidirectional pumping

Wei Wang,*[abc] Ivan Tanasijevic,[de] Jinsong Zhang,[a] Eric Lauga,[d] and Itai Cohen*[acfg]

[a]Laboratory of Atomic and Solid State Physics

[b]Sibley School of Mechanical and Aerospace Engineering

[c]Kavli Institute at Cornell for Nanoscale Science

Cornell University, Ithaca, NY, USA 14850

[d]Department of Applied Mathematics and Theoretical Physics

University of Cambridge, Cambridge, CB3 0WA, UK

[e]The Institute for Artificial Intelligence Research and Development of Serbia

[f]Department of Physics, [g]Department of Design Technology

Cornell University, Ithaca, NY, USA 14850

* Corresponding authors: ww459@cornell.edu, itai.cohen@cornell.edu

Supplementary Information

Swept area

In cilial pumping, the swept area is basically proportional to the pumping efficiency (*1*). Therefore, we need to maximize the swept area of the cilium to get the best pumping efficiency. As shown in the schematic in Supplementary Fig. 2, the Swept area (S) can be expressed as:

$$S = S_1 + S_2 - S_3 - S_4 \tag{S1}$$

with $S_1 = \frac{\theta_{2,i}-\theta_{2,f}}{2}L_2^2$, if $L_3 > L_1$, $S_2 = \frac{\theta_{1,i}-\theta_{1,f}}{2}L_3^2$, if $L_3 <= L_1$, $S_2 = \frac{\theta_{1,i}-\theta_{1,f}}{2}L_1^2$, $S_3 = \frac{\theta_{2,i}-\theta_{2,f}}{2}L_2^2$, if $L_4 > L_1$, $S_4 = \frac{\theta_{1,i}-\theta_{1,f}}{2}L_4^2$, if $L_4 <= L_1$, $S_4 = \frac{\theta_{1,i}-\theta_{1,f}}{2}L_1^2$. where $\theta_{1,i}$, $\theta_{1,f}$, $\theta_{2,i}$, $\theta_{2,f}$ are the initial and final angles of Hinge 1 and Hinge 2.

Assuming the initial hinge angles are larger than the final angle, the cilium can not penetrate the substrate and itself. The boundary conditions can be expressed as:

$$\theta_{1,i} >= \theta_{1,f}, \theta_{2,i} >= \theta_{2,f}, 0 <= \theta_1 <= \pi, -\pi <= \theta_2 <= \pi, L_1\sin(\theta_1) + L_2\sin(\theta_1+\theta_2) > 0 \tag{S2}$$

Therefore, we can find the maximal swept given a fixed cilium length ($L = L_1 + L_2$). The maximal swept area, normalized by the square of the cilium length, is found to be 0.8, with $\theta_{1,i} = 2.3$, $\theta_{1,f} = 2$, $\theta_{2,i} = 0$, $\theta_{2,f} = 0$, and $L_1 = 0.55L$. Given that the curvature change of the SEAs of about 1 to 2 μm^{-1}, we set the hinge length to 3.5 μm in this paper. Besides, the maximal swept area is not sensitive to the relative length ratio of the two hinges, therefore, we set the length of the two hinges to be equal for simplicity, which will give a maximal swept area of about 0.75. This ideally gives a 6% difference within the error bar of the pumping performance in Fig. 2.

Torque estimation

Here we aim to estimate the maximal frequency of actuation such that for lower frequencies the internal elastic stresses in hinges will suffice to force a full deformation of the cilium. For calculating the hydrodynamic drag, we approximate the cilium (see Fig. 1A) as two nearly flat disks of radius $L/4$, where L is the length of a cilium. Such a disk moving with velocity V at low Reynolds number experiences a drag force

$$F = 4\mu LV, \tag{S3}$$

as an asymptotic case of an oblate spheroid (*2*). Maximal instantaneous torque exerted by the fluid is achieved when the cilium is completely straight performing its power stroke. During this motion, it would need to swipe the angle close to 2 radians to perform a full range of motion during time $1/(4f)$ where f is actuation frequency since there are 4 parts of each actuation cycle that each lasts approximately the same (see Fig.1B). These assumptions yield the following estimate of fluid torque T_f that needs to be overcome

$$T_\mathrm{f} = 20\mu L^3 f. \tag{S4}$$

On the other hand, the hinge torque T_h can be approximated by the formula EI/L_h, where E is Young's Modulus, I denotes the hinge's moment of inertia, and L_h is its length. We use this value to estimate the internal torque produced by the hinge during actuation.

By employing the parameters used in this study with L of 50 µm, E of 152 GPa, and L_h of 3.5 µm, we reach the estimates of about 7.6× 10^{-14} Nm for the hinge torque and the fluid torque of about $T_\mathrm{f} = 2.5 \times 10^{-15} f$ Nm. Therefore, the fluid torque reaches the same order as the hinge torque at about 3.0 Hz and is equal to the hinge torque at about 30.4 Hz.

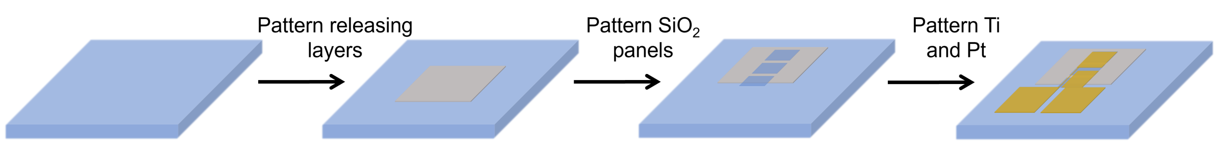

Supplementary Fig. 1 Fabrication process of the hinged cilium. We use the standard photolithography to fabricate the cilium. The fabrication process involves the pattering of releasing layers, SiO_2 panels, and Ti, Pt layers.

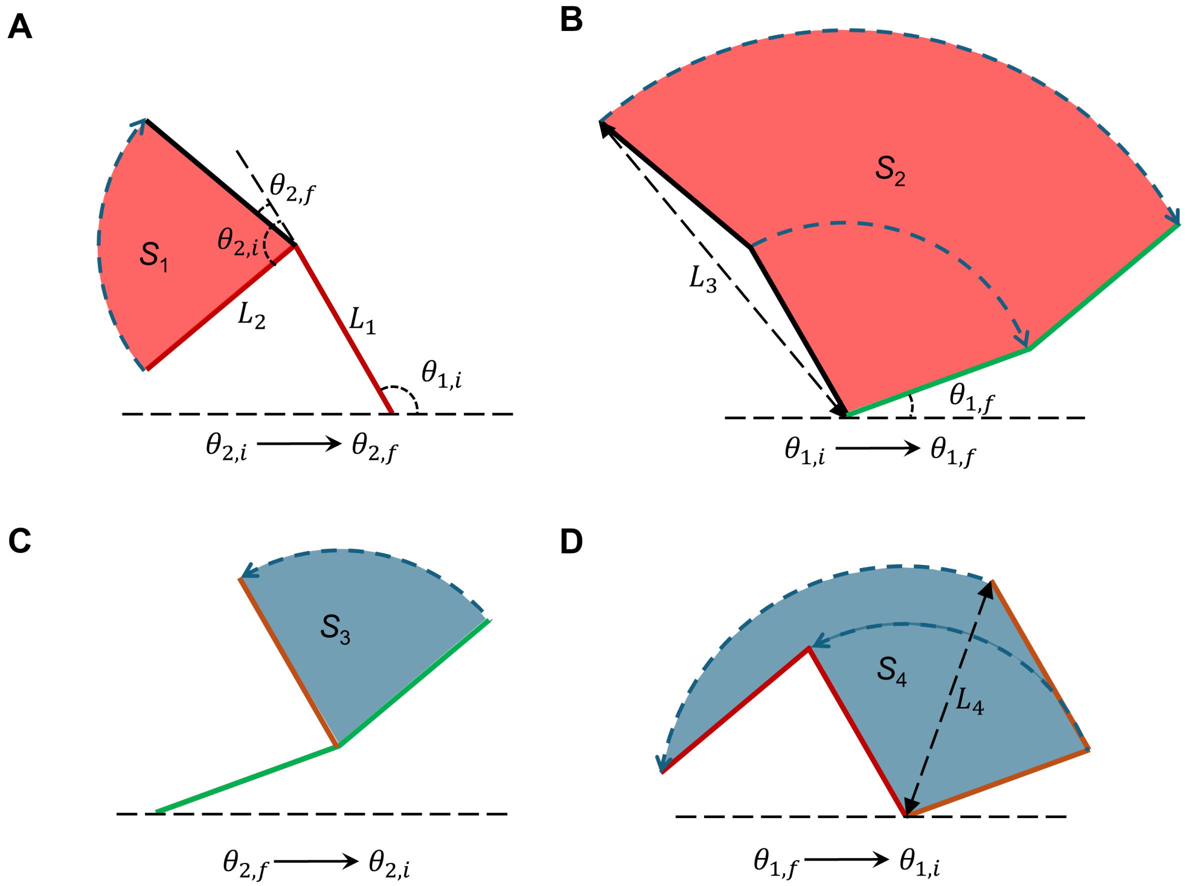

Supplementary Fig. 2 Swept area of the hinged cilium. Assuming the cilium undergoes a shape-shifting from (A) to (D), the swept area, indicated by the trajectory of the tip, is S_1+S_2-S_3-S_4. Reversing the shape-shifting cycle will reverse the sign of the swept area.

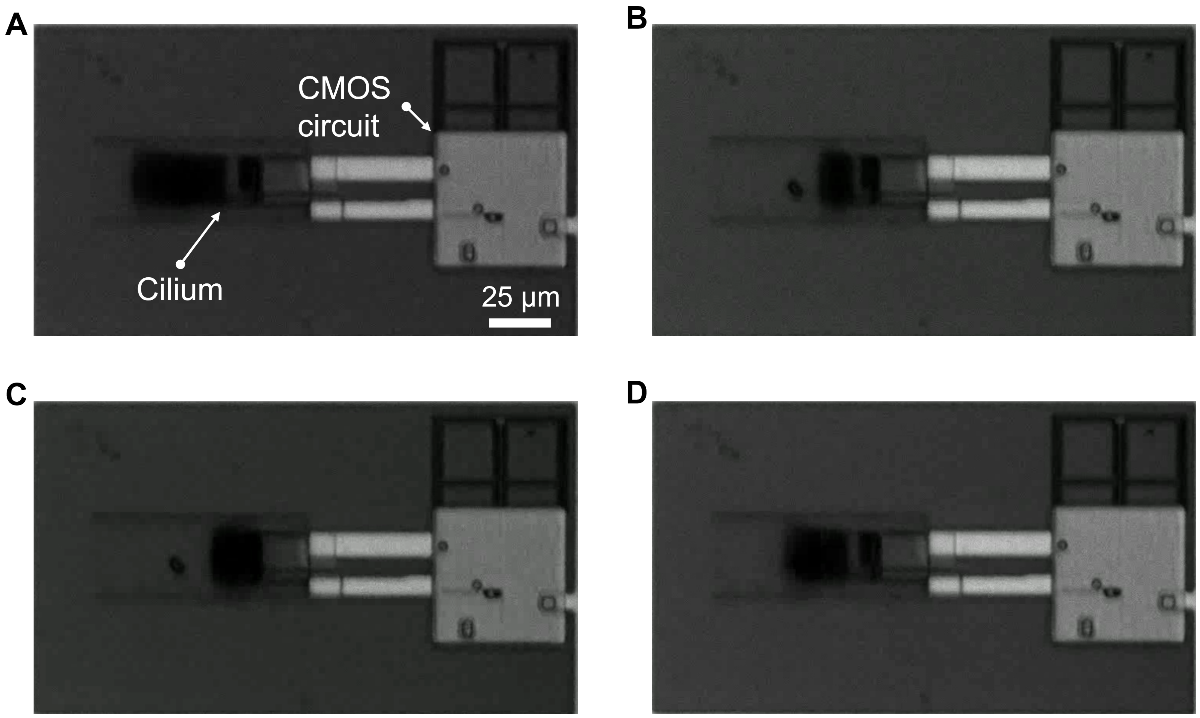

Supplementary Fig. 3 CMOS circuit integrated hinged cilium. (A-D) show the shape-shifting sequence of the hinged cilium in one actuation loop. (A) Both hinges flatten. (B) Hinge 1 bends up. (C) Hinge 2 bends up. (D) Hinge 1 flattens.

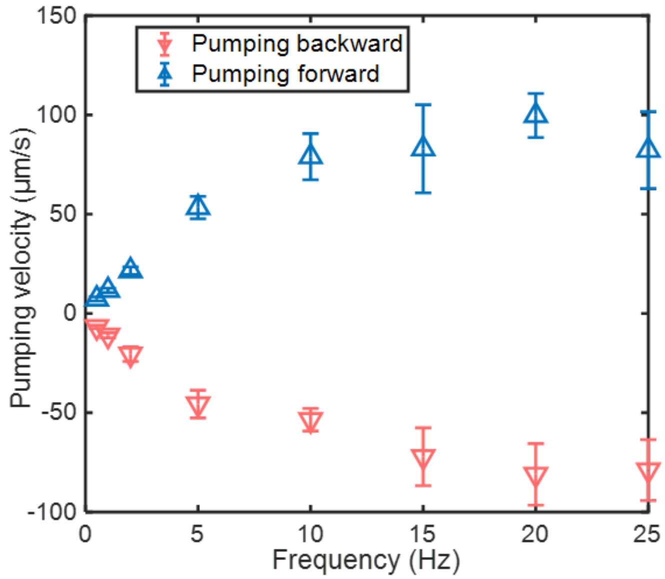

Supplementary Fig. 4 Pumping velocity of the hinged cilia. The relationship between the actuation frequency and the pumping speed of the hinged cilia.

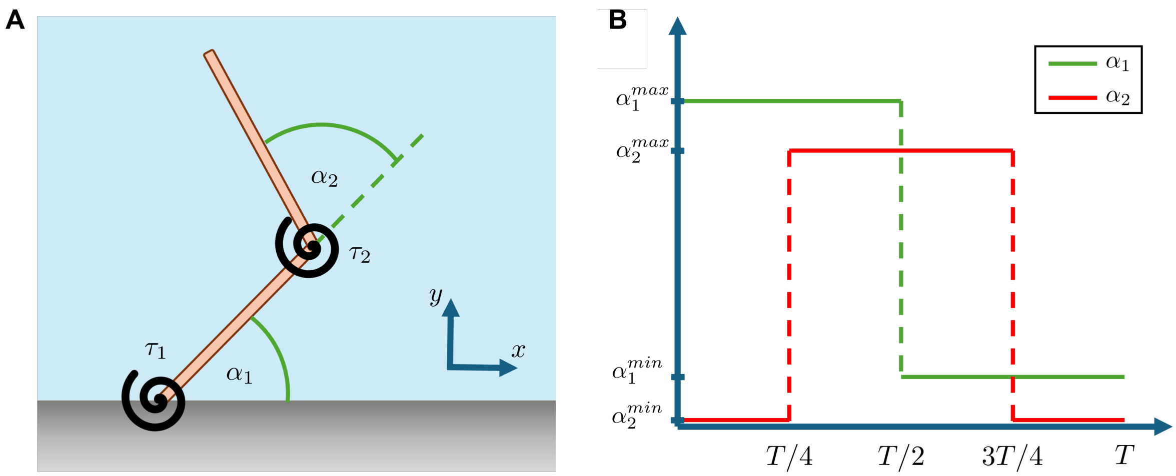

Supplementary Fig. 5 Illustration of the theoretical model of a hinged cilium. (A) The cilium is modeled as rigid rods connected by torsional springs. (B) The torsional springs oscillate between the prescribed angle ranges with a $\pi/2$ phase delay.

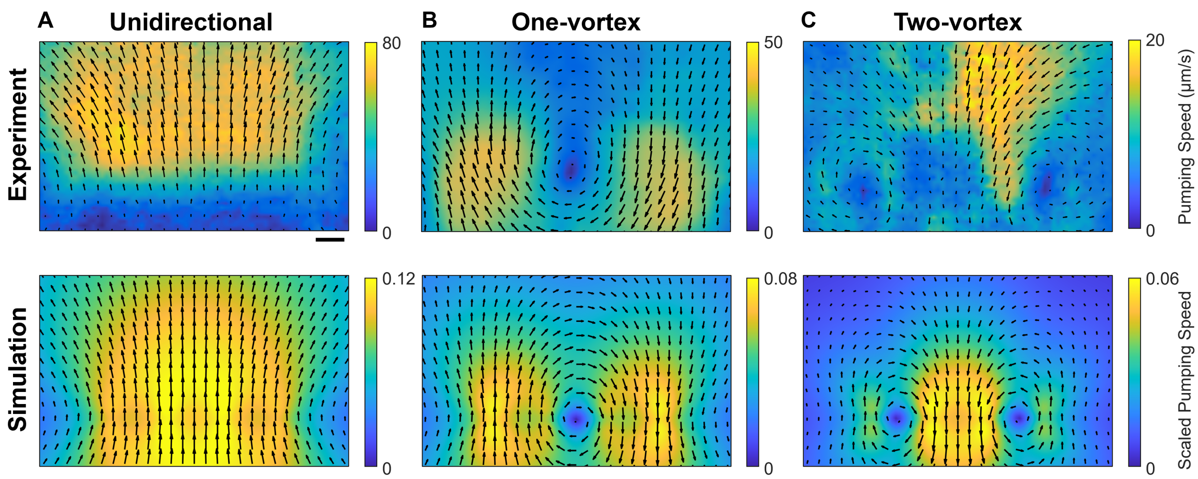

Supplementary Fig. 6 The experimental and simulation velocity fields from a cilia array with four hinged cilia. (A) Unidirectional flow. (B) Flow with one vortex. (C) Flow with two vortices. Scale bar: 25 µm.

References

1. Wei Wang, Qingkun Liu, Ivan Tanasijevic, Michael F Reynolds, Alejandro J Cortese, Marc Z Miskin, Michael C Cao, David A Muller, Alyosha C Molnar, Eric Lauga, et al. Cilia metasurfaces for electronically programmable microfluidic manipulation. *Nature*, 605(7911):681–686, 2022.

2. S. Kim and S.J. Karrila. *Microhydrodynamics: Principles and Selected Applications*. Butterworth - Heinemann series in chemical engineering. Dover Publications, 2005.